IJCRT.ORG ISSN : 2320-2882

INTERNATIONAL JOURNAL OF CREATIVE RESEARCH THOUGHTS (IJCRT)

An International Open Access, Peer-reviewed, Refereed Journal

GRAPHENE PREPARATION METHOD

Tarun Radadiya

PG Data Science Student of Amity University (India), Data Analyst Student of eCornell University (USA), Team Lead in Paytm

Abstract: Over the past decade, Graphene has advanced rapidly as one of the most promising materials changing human life. Development of production-worthy synthetic methodologies for the preparation of various types of Graphene forms the basis for its investigation and applications. Interest in Graphene centres on its excellent mechanical, electrical, thermal and optical properties, its very high specific surface area, and our ability to influence these properties through chemical functionalization. There are a number of methods for generating Graphene and chemically modified Graphene from graphite and derivatives of graphite, each with different advantages and disadvantages. Here we review the use of colloidal suspensions to produce new materials composed of Graphene and chemically modified Graphene. This approach is both versatile and scalable, and is adaptable to a wide variety of applications.

Keyword **- Preparation of Graphene, Graphene application**

I. INTRODUCTION

Graphene is a single atomic layer of carbon atoms tightly packed in a two-dimensional honeycomb lattice. The novel material has generated great interest throughout the scientific and technological community because of its remarkable properties and numerous potential applications. However, obtaining pure and highly ordered Graphene has been a challenge. Small quantities of ultrahigh-quality Graphene have been isolated through an unwieldy and time-consuming process involving the mechanical exfoliation of highly oriented pyrolytic graphite. Alternative methods require substrates or graphite to create atomically-thin sheets, and these techniques involve multiple steps, expensive substrates, or non-ambient conditions. Furthermore, the sheets produced by these alternative methods exhibit defects, disorder, and oxygen functionalities that have a detrimental effect on the properties of Graphene.

Preparation of Graphene films

100 ml Graphene NMP dispersion with a concentration of 0.14 mg ml-1 was filtered by Nylon membrane with 220 nm in pore size. The obtained thin Graphene paper was dried at 60 °C for 36 hours.

Structural characterization

The morphology of natural graphite, TEA-GIC, EG, and graphene films was examined by field-emission scanning electron microscopy (SEM, Hitachi S-4800). Atomic force microscope (AFM) characterization was conducted with a Veeco Dimension 3100V scanning probe microscope at ambient conditions using the tapping mode. The sample for AFM measurement was prepared by dip-coating. A mica sheet was immersed in 0.001 mg ml-1 graphene NMP dispersion for 5 minutes to adsorb a thin layer of graphene flakes. After that, it was immersed in de-ionized water for another 5 minutes to remove unadsorbed graphene. Powder X-ray diffraction (XRD) patterns of natural graphite, TEA-GIC, and EG were recorded with Bruker AXS D8 Advanced X-Ray Diffract meter. The electrical conductivity of graphene film was measured by a physical property measurement system (PPMS) (Quantum Design Model-9). The structural information of natural graphite, TEA-GIC, and EG was also obtained from Fourier transform infrared spectra (FTIR), which were acquired using a Thermal Nicolet 6700 FTIR spectrometer. Raman and X-ray photoelectron spectroscopy (XPS) measurements were carried out using a Raman microscope (Thermo Scientific DXR) with 532 nm laser and Multifunctional XPS (Shimadzu Axis Utltradld), respectively.

II. PREPARATION OF GRAPHENE

The process of preparing graphene consisted of three steps, as shown schematically in Figure 1: (a) aqueous phase intercalation of natural graphite to produce TEA-GIC, (b) microwave irradiation to obtain EG, and (c) sonication of EG in organic solvents such as NMP, DMF and GBL to obtain graphene. The TEA-GIC was produced by tip sonication (855 W) of graphite in aqueous solution containing thionin acetate salt, sodium hydroxide and TEA. Thionin cations entered graphite galleries after the intercalation of TEA to stabilize TEA-GIC while sodium hydroxide provided hydroxide anions for subsequent elimination of TEA. The TEA-GIC was further microwave irradiated in air. The release of gaseous species induced by the decomposition of TEA led to expansion of graphite. After mild sonication in organic solvent, this EG could be readily exfoliated into dispersive graphene sheets. The single-cycle yield of graphene was 5% determined by weighing the residue after filtration of the graphene dispersion. This value is four times higher than that obtained by liquid-phase exfoliation of graphite in NMP for half an hour [63] and even higher than that obtained by treatment of graphite using the same method for 460 hours [2]. The yield of graphene can be further improved with unexfoliated graphite recycled to repeat the above process.

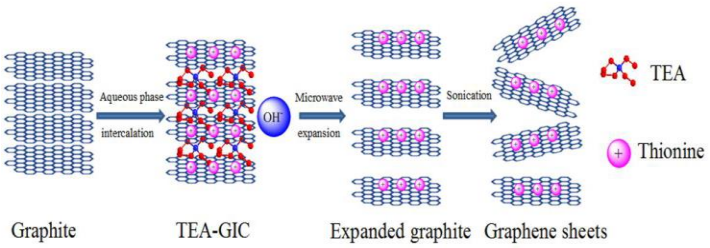

Figure:-1. Illustration of experimental procedure for preparation of graphene by liquid phase intercalation and exfoliation of graphite.

We observed the Tyndall effect with a laser passing through the dispersion, indicating that the graphene sheets were quite evenly dispersed in the solvent. This suspension was stable without noticeable sediments even after being shelved for one month. The whole experimental processes lasted only one day and were quite straightforward to implement and control

III. EPITAXIAL GROWTH ON SIC

Graphene, a two-dimensional array of carbon atoms in honeycomb lattice, has been theoretically studied for decades in terms of the fundamental building block of carbon based materials, such as graphite and carbon nanotubes [3,4]. However, the first observation of freestanding graphene was not realized until 2004 with mechanical exfoliation method by peeling graphene flakes from a bulk graphite crystal onto SiO2 substrate [5]. Since then, a variety of novel properties, including quantum Hall effects, and relativistic quasiparticles with a group velocity of 1/300c (where c is the speed of light) [6-8] have been observed. These unique properties, together with the high values of conductance, mobility, and mechanical strength [6,9, and 10] make graphene a promising material for a wide variety of new technological applications [11-13], such as post-CMOS digital electronics, single-molecule gas sensors, spintronic devices, etc.

To realize the application potential of graphene, reliable methods for fabricating large-area single-crystalline graphene domains are required. The most promising approach in this respect seems to be the controlled graphitization of SiC surfaces [6,14]. In this method, single layer and/or multilayer graphene can be grown by sublimating Si atoms from SiC substrates at high temperature. In spite of a lot of efforts devoted to the improvement of synthesis methods to form large areas of uniform, electronic grade graphene by the thermal desorption process is still very challenging. In this paper, we will give a short review on the current state of epitaxial graphene research, and we will then introduce a new developed synthesis method, the "**face-to-face**" method, which allows preparing good quality monolayer, bilayer and three layer epitaxial graphene samples on 6H-SiC(0001) substrate.

Although growing thick graphite samples on SiC has been a well-known process for many years [15-17], it is not until recently that the thickness was pushed down to few layers and a full characterization of the high quality graphene sample has been carried out [6,18,19]. The growth of epitaxial graphene on SiC is based on thermal decomposition of the SiC substrate. Both e-beam heating as well as resistive heating have been used, but no difference seems to arise from the different heating methods [20]. In order to avoid contaminations the heating is usually performed in ultra-high vacuum (UHV) environment. Similar results have been observed for high and/or low base pressure growth but so far no comparative study about the influence of the background pressure in the vacuum chamber has been conducted. From the molar densities one can calculate that approximately three bilayers of SiC are necessary to set free enough carbon atoms for the formation of one graphene layer [20]. The growth of graphene can take place on both the (0001) (silicon-terminated) or (000-1) (carbon-terminated) faces of 4H-SiC and 6H-SiC wafers. The main difference lies in the sample thickness that one can achieve. In the case of silicon face, the growth is slow and terminates after relatively short time at high temperatures giving rise to very thin samples, up to a monolayer. On the contrary, in the case of the carbon face, the growth does not self-terminate giving rise to relatively thick samples (approximately 5 up to 100 layers) [21] with larger orientational and turbostatic disorder [22-24].

IV. EPITAXIAL GRAPHENE ON SIC (0001) FACE

Hydrogen etching is performed as a normal routine of pretreatment to remove scratches from polishing and oxides and leave a surface with highly uniform, atomically flat terraces. Although it is believed that larger graphene sheets should be obtained with a smoother graphitization surface [25], the relevance of pre-graphitization SiC surface to better graphene order has not been substantiated. Recently, the relation between initial surface morphology and sample quality has been discussed by Ohta *et al*. [26]. They observed the formation of graphene on SiC by Si sublimation in Ar atmosphere, and identified two types of monolayer graphene with different shapes. It was noticed that large graphene sheets preferred to grow along the triple bilayer SiC steps, while narrow graphene ribbons formed following the surface of single bilayer SiC height. The dependence between growth mechanisms and initial surface morphology indicates the effects of H2 etching on the formation of graphene. The result suggests that by minimizing the number of single bilayer SiC steps with H2 etching, better graphene sample should be achieved.

To compensate the depletion of Si during the pre-cleaning process, external Si flux is applied before the SiC substrate is heated to higher temperature to grow graphene. A number of surface reconstructions prior to graphitization have been observed and studied by low-energy electron diffraction (LEED) [16,17]. LEED patterns obtained at different stages during the growth of graphene. The initial Si-rich (3 × 3) phase can be obtained by exposing a well-outgassed SiC surface to a Si flux at a temperature of 800 °C. A subsequent 5 min annealing at 1000 °C in the absence of Si flux gives rise to the sharp pattern shown in panel (a), corresponding to the 1 × 1 spots of SiC. Further annealing for 5 min at 1100 °C produces the ($\sqrt{3} \times \sqrt{3}$) R30 reconstruction shown in panel (b). Finally, the complex (6×3 √ 6×3) R30 pattern shown in panel (c) appears after 10 min annealing at 1250°C, demonstrating the formation of graphene. In different experiments, the annealing temperature can be various. It should be noticed that the first carbon layer grown on the Si-face of SiC, referred as buffer layer, is not graphene. Although the atomic arrangement of this layer is identical to that of graphene, however, unlike graphene, one third of the carbon atoms of this layer are covalently bonded to the underlying Si atoms of the topmost SiC layer. The π-band is developed between buffer layer and following graphene layers.

Compared to the Si-face, graphene on SiC (000-1) face has been less studied, due to the early conclusion that C face films were of poor quality and rotationally disordered [29]. However, a detailed study indicates that the azimuthal disorder detected by low energy electron diffraction (LEED) is not random [30]. In multiple layer graphene grown on SiC (000-1) face, epitaxial layers can orient either in the 30° phase or in the ±2° phase with respect to the substrate, which is indicated. The different orientations between adjacent layers cause them to decouple form each other, forming a system which preserves the transport and electronic properties of free-standing monolayer graphene [14,31]. Due to this unique property, C-face grown graphene attracts more and more attention. The major problem with the growth of epitaxial graphene on C-face of SiC is the lack of precise control in sample thickness. The controllability has been demonstrated by Camara *et al*. [30] lately.

V. THE FACE-TO-FACE METHOD

As indicated in the review above, high quality epitaxial graphene sheets in large scales now can be achieved. However, the growth process gets more complicated because more parameters are introduced into the system, such as annealing atmosphere. In the following part, we will report a new synthesis method, the "face-to-face" method, which is straightforward, simple, and economical, and yet yields good quality graphene of large length scales. Here two SiC substrates are placed one on top of the other face to face, with a small gap in between, and are then heated simultaneously. The grown samples show larger terraces sizes and better homogeneity than the one obtained by annealing SiC in ultra high vacuum, as demonstrated by LEED, atomic force microscopy (AFM), angle resolved photoemission spectroscopy (ARPES) and Raman measurements performed on the as grown sample. Moreover we show that the graphene thickness can be easily and well controlled by changing the annealing temperature. The results suggest that the method has potential for efficient production of graphene base devices. Figure 2(a) shows schematic diagram of our vacuum furnace with a base pressure ≤ 1×10-6 Torr, maintained by 30 *l*/s hybrid turbo pump (HTP). Two rectangular pieces of SiC are stacked in pairs with spacers of Ta foil at the edges for a 25 micron gap between the two inner surfaces, the key idea of this method from which the name "face-to-face". The pieces are oriented so that the Si-terminated surfaces face each other. The two ends of the stack are wrapped by "L"-shaped pieces of Ta foil at each end and connected to electrodes allowing simultaneous parallel resistive heating.

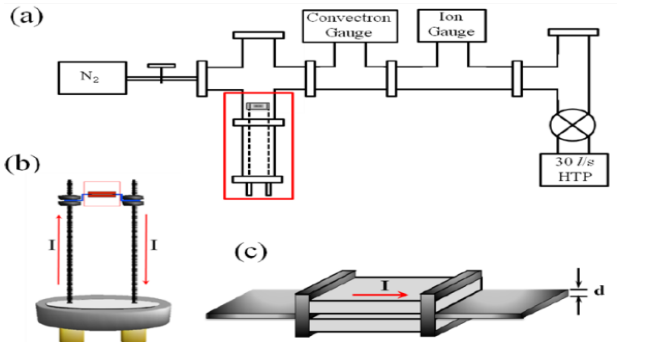

Figure:-2 (a) Schematic view of the configuration used for "*face-to-face*" growth method setup; (b) magnified view of the sample setup highlighted in panel (a), where rectangulars in red represent SiC substrates, and lines in blue represent Ta foil; (c) magnified view of mounted SiC substrates highlighted by red lines in panel (b), the distance between Si-face of the two substrates equals to the thickness of Ta foil (d = 25μm). SiC substrate is in light gray and Ta foil is in dark gray.

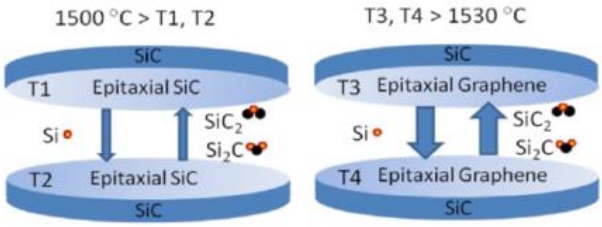

Figure:-3 two-step growth model for preparing epitaxial graphene Panel (b) and (c).

Temperature was monitored by an infrared optical pyrometer set to an emissivity of 0.96. The simple geometry of this method results in two important effects. First, at temperatures below 1500 °C (before graphene growth has begun), both pieces act as sources as well as sinks of SiC on the opposing surface (Figure. 3a). Large atomically flat terraces form during this annealing process without careful hydrogen etching which is usually applied in other approaches as a pre-treatment for graphene preparation. By first creating large, flat substrate terraces, the eventual graphene layer can have similarly large terrace sizes. Second, the close proximity of the two surfaces partially traps Si atoms which sublimate from each heated surface, increasing the local partial pressure of Si within the gap. The pressure of Si vapor next to the surfaces of the SiC crystals restricts the net rate of Si sublimation from the substrates Figure. 3) and allows large pieces of graphene to be formed as described above. Thus, the same effect as in previous methods aiming to improving graphene annealing conditions by reducing Si sublimation (ambient pressures of Ar or disilane) is achieved in a very simple manner. We note that as Si can escape from the gap near the edges of the pieces, control of the Si sublimation from the edge of the substrates is reduced, resulting in thicker and poorer quality of graphene around the edges.

(a) **(b)** **(c)**

Figure:-4 (a–c) LEED patterns with a primary energy of 180 eV, obtained at four different stages during the growth of sample

(a) 1 × 1 spots of SiC, after a 5 min anneal around 1000 °C followed by the initial cleaning procedure under Si flux. (b) ($\sqrt{3} \times \sqrt{3}$) R30 reconstruction, after 5 min around 1100 °C. (c) ($6\sqrt{3} \times 6\sqrt{3}$)R30 reconstruction, after 10 min around 1250 ° C. The substrates used in the experiments were cut into 4×6 mm² using a diamond saw from n-type 6H-SiC (0001) single crystalline wafers1. The substrates were degassed at 700 °C for 4 hours followed by annealing at elevated temperatures of 1530 – 1700 °C. During the initial growth stage at 1500 °C, epitaxial SiC layers are nucleated on the two substrates creating atomically flat SiC with large terrace sizes. The sublimation of Si prevails over decomposition of SiC with higher annealing temperature than 1530 °C, which results in the formation of micrometer scale graphene sheets. As in other methods, higher temperatures lead to thicker, or more layers, of graphene. In the present method, 1530 °C results in single layer graphene, and 1700 °C results in triple layer graphene.

VI. CHEMICAL REDUCTION OF GRAPHITE OXIDE

The scheme for the two classes of rGO-based thin films discussed in this Review is illustrated in Figure 6. Type one are pure rGO films, which consist of a percolating network of sheets lying flat on a substrate surface. Type two are composite films consisting of rGO as the filler and polymer or ceramic as the host material. The starting point for the fabrication of these films is the oxidation of graphite, which readily exfoliates in water, forming a colloidal suspension of GO. For electronic and optoelectronic applications discussed here, GO, which is electrically insulating, must be reduced to become electrically conductive.[31] Various methods of reduction have been reported, resulting in varying degrees of restored electrical conductivity. Similarly, thin-film-deposition techniques of GO/rGO influence the degree of coverage, number of layers, and surface morphology giving rise to a variety of properties. In the following Sections, synthesis, dispersion, reduction, and deposition of GO are discussed.

Synthesis of graphite oxide can be achieved by placing graphite in one or more concentrated acids in the presence of an oxidizing agent. Graphite oxide was first prepared almost 150 years ago by Brodie, who treated graphite repeatedly with potassium chlorate and nitric acid.[32] This method was modified by several investigators including Staudenmaier[33] and Hamdi[34] who used a mixture of sulfuric acid and nitric acid with potassium chlorate. Hummers and Offeman[35] later demonstrated a less hazardous andmore efficientmethod for graphite oxidation, which involves a mixture of sodium nitrate, potassium permanganate, and concentrated sulfuric acid. These and their modified versions are presently the most commonly used methods for the oxidation of graphite.[36–39] Othermethods such as electrochemical oxidation of graphite have also been reported.[40]

Graphite oxide in water hydrolyzes to form thin platelets, which are negatively charged. While Brodie[17] remarked that the platelets were ‘‘extremely thin,’’ it was about 100 years later when Boehm et al.[41] concluded that the thinnest graphite oxide platelets consisted of single-carbon-thick layers. Today, the existence of monolayers of graphite oxide is widely acknowledged and recognized as graphene oxide (GO).[42,31] The term ‘‘platelets’’ is often used to describe thick multilayers of GO or rGO, while ‘‘sheets’’ usually indicate a monolayer to few layers.[43] Individual sheets of GO can be viewed as graphene decorated with oxygen functional groups on both sides of the plane and around the edges as described by Lerf et al.[44,45]

(Figure:-6). Due to ionization of carboxyl groups, which are primarily present at the sheet edges (Figure:-6), GO can be electrostatically stabilized to form a colloidal suspension[46] in water, alcohols, and certain organic solvents[47,48] without surfactants. Exfoliation of graphite oxide into individual sheets can be facilitated by ultrasonic agitation[50] or rapid heating[49,51] but excessive ultrasonication can result in decrease of lateral dimensions.[52,53] Oxidation of graphite results in a brown-colored viscous slurry, which contains graphite oxide and exfoliated sheets along with nonoxidized graphitic particles and residue of the oxidizing agents. After repeated centrifugation, sedimentation, or dialysis, salts and ions from the oxidation process can be removed from GO suspensions (see for example, Ref. [54-57]). To achieve a suspension of monolayer GO, nonoxidized graphitic particles and thick graphite oxide platelets are precipitated out by further centrifugation. Suspensions of GO flakes that are monodispersed according to their lateral size can also be obtained by density-gradient centrifugation.[53].

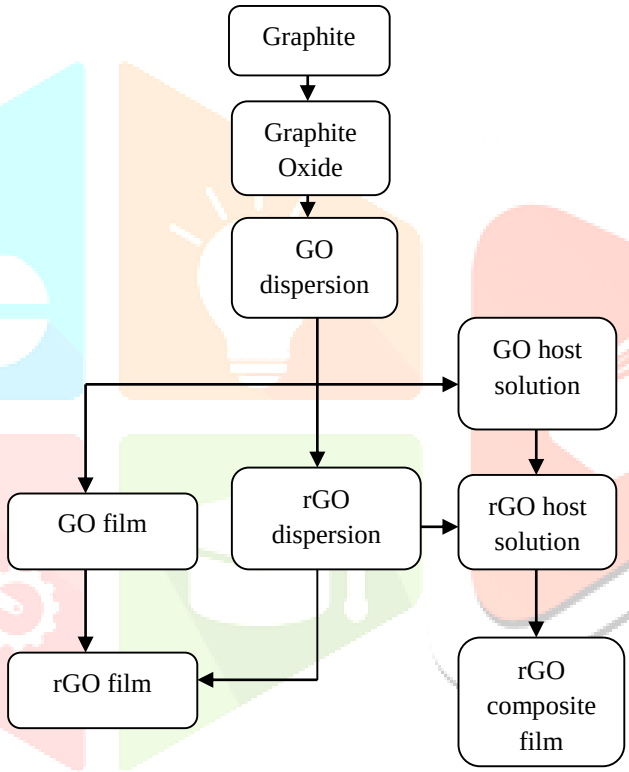

Figure:-5 Process scheme for fabricating rGO-based thin films

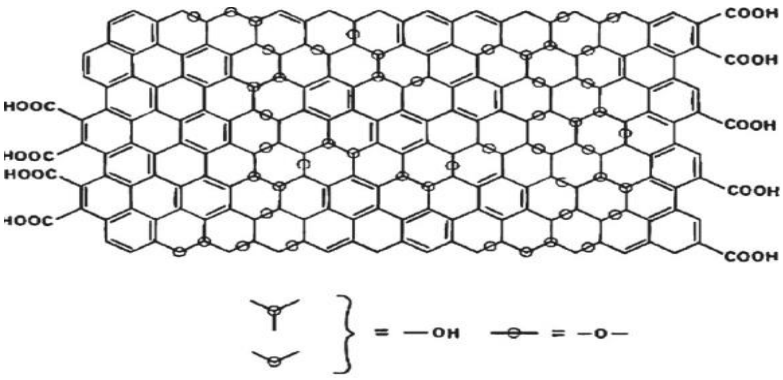

Figure:-6 Chemical structure model of GO.

Position of oxygen functional groups are indicated by circles. The functional groups are attached on both sides of the graphene sheet.Reproduced with permission from [94]. The thickness of a monolayer GO sheet is approximately 1–1.4 nm, which is thicker than an ideal monolayer of graphene (thickness _0.34 nm) due to the presence of functional groups and adsorbed molecules [44,58] Since the functional groups make GO strongly hydrophilic, multilayered GO contains trapped water molecules between the layers.[46,58,59] Studies have shown that these molecules can be partially removed from the structure during thermal reduction [58,60] Despite the difference in their optical properties, like pristine graphene,[61,62] GO sheets are also readily visible on Si substrates with 300-nm SiO2 [63] Furthermore, high-contrast visualization of GO on arbitrary substatrates can be achieved by fluorescence quenching microscopy.[64,65] The maximum lateral size of GO sheets is dependent on the size of initial graphite crystals, but the average size can be adjusted to some degree by the extent of oxidation procedure[66] or by ultrasonication.[52,53] Large and small GO sheets observed with optical and atomic force microscopy (AFM), respectively, demonstrate the wide range of lateral sizes. By using large graphite crystals as the starting material and employing a multistep oxidation process, GO sheets as large as 3mm have been synthesized.[66] Due to the ease of identification on SiO2/Si substrates and their large lateral size, GO sheets can be contacted with metal electrodes for electrical studies using standard lithographic techniques.[67] On the other hand, GO sheets having lateral sizes of few nanometers have also been observed after extensive ultrasonication.[53]

VII. REDUCTION OF GRAPHENE OXIDE

There are a number of routes for reduction of GO, as briefly summarized in recent reviews.[68,69] Chemical methods involve exposure of GO to reducing chemicals such as hydrazine (hydrazine monohydrate,[40,66,67]dimethylhydrazine, [29,52] and anhydrous hydrazine[70]),hydrides(sodiumborohydride[71–74] and sodium hydride[75]), hydroquinone,[71,76] and p-phynylene diamine.[77] Reduction of GO also occurs in strongly alkaline environments[78] and in supercritical water.[79] Thermal reduction of GO is typically achieved above 200 8C in inert or reducing environments and becomes more efficient at higher temperatures.[88,89,80] It should be noted that in the presence of oxygen, GO decomposes quickly at high temperatures[32] and gradually at lower temperatures (<200 8C). Annealing GO in NH3 atmosphere above 300 8C results in reduction as well as N doping via formation of C-N bonds.[81] Efficient chemical reduction of GO is achieved in solution, since both sides of the sheets can interact with the reducing agent while in thin films only the exposed regions are reduced.[55,82] Hydrazine is effective for the removal of in-plane functional groups such as epoxy and hydroxyls but leave the edge moieties such as carboxyl and carbonyl intact.[84,56,83] Gao et al.[85] demonstrated that these residual edge groups can be removed by additional exposure to concentrated H2SO4 after the initial reduction treatment. As an alternative to chemical methods, hydrogen plasma treatment has been also shown to result in efficient reduction.[68] Other routes include electrochemical reduction,[86–88] photocatalytic reduction,[89] and flash conversion,[91] but no comparative studies on their reduction efficiencies have been conducted.

VIII. CHEMICAL VAPOR DEPOSITION

The “top-down” exfoliation technique has been widely used to produce two-dimensional atomic crystals including not only graphene but also many other 2D materials, as BN and MoS2[92]. This process of producing graphene sheets has been found to be reliable and easy and has attracted the immediate attention of the scientific community. The best quality graphene, in terms of structural integrity, has been obtained by this method up to now. However, only flat graphene flakes (tens of microns in size) can be produced and the number of exfoliated layers is not easily controlled. As in most practical applications conceived for graphene, including microelectronics, optoelectronics (solar cells, touch screens, liquid crystal displays), graphene based batteries, super-capacitors and thermal control , large area and high quality with low structural defects graphene is needed [93] other methods should be developed. The preparation of graphite from heterogeneous catalysis on transition metals has been known for years. Independently of this, the first report on CVD synthesis of few layer graphene (FLG) was published in 2006 [94]. Since then, the CVD “bottom-up” synthesis has evolved to scalable and reliable production method of large area graphene. Synthesis of large area and high quality graphene has been demonstrated by this method [95,96]. But comparing CVD graphene properties to exfoliated graphene, the latter goes on exhibiting better quality so far.

Currently the growth and development of high quality, large-area CVD graphene on catalytic metal substrates is a topic of both fundamental and technological interest. Since the large-scale graphene films synthesized so far are typically polycrystalline, the research effort is aimed to control the domain size, the number of graphene layers, the density of grain boundaries, and the defects and so on. For graphene materials to realize the promise of “graphene based applications”, it is clearly necessary to solve those problems, preventing defects in fabricated devices.

CVD synthesis and growth of graphene

There exist comprehensive review articles and books dealing with generic aspects of the Chemical Vapor Deposition. Here we are only intent on describing elemental details of CVD applied to graphene synthesis. We encourage the readers to increase their knowledge with the fundamental aspects of Vapor Deposition Processes revisiting the cited references [97-103].

CVD chemical reactions and processes

Chemical Vapor Deposition (CVD) involves the activation of gaseous reactants and the subsequent chemical reaction followed by the formation of a stable solid deposit over a suitable substrate. The energy that the chemical reaction demands can be supplied with the aid of different sources; heat, light or electric discharge are used in thermal, laser assisted or plasma assisted CVD, respectively. The deposition process can include two types of reactions: homogeneous gas phase reactions, which occur in the gas phase, and heterogeneous chemical reactions which occur on/near the vicinity of a heated surface leading to the formation of powders or films,

in each case. Though CVD has been used to produce ultrafine powders, this review article is mainly concerned with the CVD of extremely thin graphene films. So heterogeneous chemical reactions should be favoured and homogeneous chemical reactions avoided during the designed experiments. Figure:-7 shows a schematic diagram of a typical CVD process.

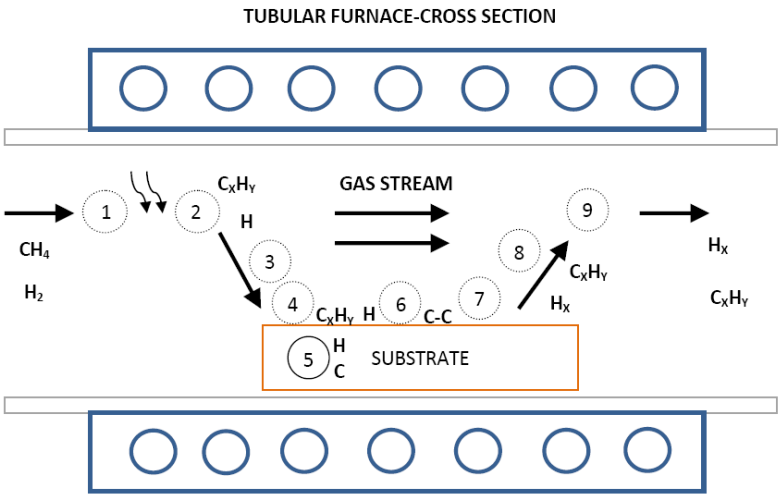

Figure:-7 (a) Schematic diagram of Thermal CVD a) and Plasma Assisted CVD b) process: case of graphene from CH4/H2 mixtures.

1. Transport of reactants by forced convection.

2. Thermal a) or plasma b) activation. Homogeneous gas reaction with particles and powder production should be avoided in graphene synthesis, controlling the kinetic parameters (P,T,n).

3. Transport of reactants by gas diffusion from the main gas stream through the boundary layer.

4. Adsorption of reactants on the substrate surface.

5. Dissolution and bulk diffusion of species depending on the solubility and physical properties of the substrate

6. Thermal activation mediated-surface processes, including chemical decomposition (catalytic), reaction, surface migration to attachment sites (such as atomic-level steps), incorporation and other heterogeneous surface reactions. Growth of the film.

7. Desorption of byproducts from the surface.

8. Transport of byproducts by diffusion through the boundary layer and back to the main gas stream.

9. Transport of byproducts by forced convection away from the deposition region.

IX. PREPARATION OF CVD-GRAPHENE.

Chemical vapor deposition (CVD) of large-area single-layer graphene on metal films was explored widely in some respects up to now. Despite the significant progress, CVD graphene is a polycrystalline film made of micrometer to millimeter size domains. To date the graphene films grown on Ni foils or films did not yield uniform monolayer graphene. In most cases, a

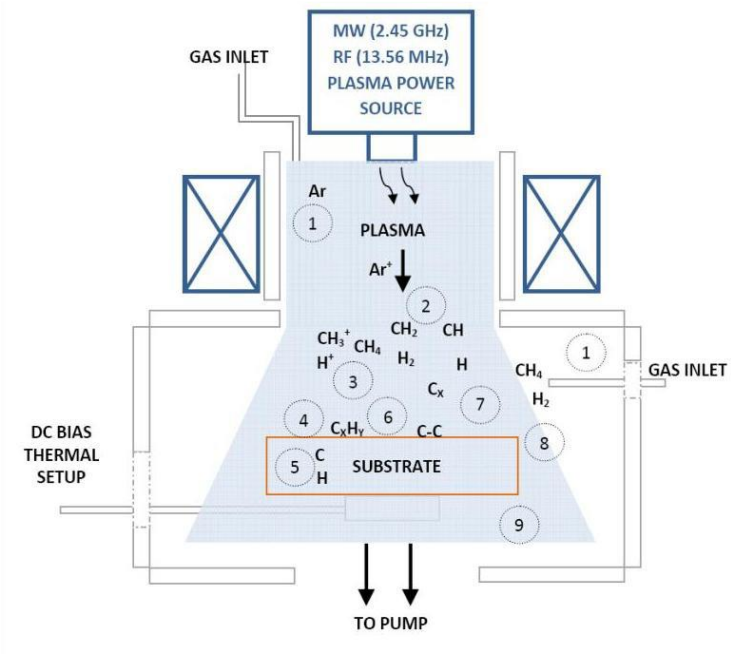

Figure:-7 (b) Schematic diagram of Thermal CVD a) and Plasma Assisted CVD b) process: case of graphene from CH4/H2 mixtures**.**

Mixture of monolayer and few layers (polygraphene) was obtained. On the other hand, it was shown that Cu is an excellent candidate for making large area, uniform thickness (95%) single layer graphene films due to the low solubility of C in Cu [165]. It was suggested and even demonstrated that the graphene growth on Cu is somehow surface mediated and self-limiting.

Processing steps

- **Heating step:** heating in controlled atmosphere the catalyst-substrate and gases (in hot wall reactors) up to the pre-process temperature.
- **Annealing step:** Maintaining the temperature and gas atmosphere so reducing the catalyst surface. This is the first chemical reaction of the whole process. It is performed to clean the catalyst surfaces and modify, as possible, the surface morphology including crystalline orientation, roughness (smoothing) and grain size of the metal catalyst. Metal evaporation should be avoided as possible.
- **Growing step:** Introduction of new precursors and growth of graphene over the catalyst substrate**.** During the growth process there are different strategies to growth the graphene film. There are one-step processes or many-step processes. During the steps is possible to modify the pressure or mix of gases, residence time, T, gas flow…It is important to take into account that depending on the nature of the catalyst (solubility, catalytic action and so on), the graphene may grow during this step or in the next one.
- **Cooling step:** After the growing step, the next step is cooling the reactor in proper atmosphere. The atmosphere commonly used is similar to that of the annealing or growing step, until the reactor temperature is under 200ºC to prevent oxidation of the catalytic surface not covered or graphene functionalization with oxygen containing groups. When working with high solubility substrates, cooling step dynamics is critical to control the growth due to the solubility dependence.
- **Final step:** Backfill with inert gases (Ar, N) up to atmospheric pressure and open the reactor chamber.

X. GROWTH KINETICS AND REACTION MECHANISMS

Hydrocarbon based reactants, being methane (CH4) the most mentioned, were commonly used as C source. Due to strong C-H bonds in methane molecule (440 kJ/mole) its thermal (non-catalytic or non plasma activated), decomposition (step 2 in fig. 1) occurs at very high temperatures (>1200 ºC) [104]. This high temperature is not easily obtained in a typical thermal CVD setup. To reduce the temperature of methane's decomposition different transition metal catalysts (e.g., Fe, Co, Ni, Cu) were widely used. This catalytic behavior is observed when growing CVD graphene on metals at low temperatures (<900ºC) in a greater or lesser extent. Therefore, non catalytic activation can be considered negligible working in thermal systems [105]. On the other hand, in the case of plasma assisted CVD, the activation and decomposition of gases prior to reach the substrate is effectively performed, but surface diffusion is a thermal-mediated process and plays a fundamental role in growth kinetics.

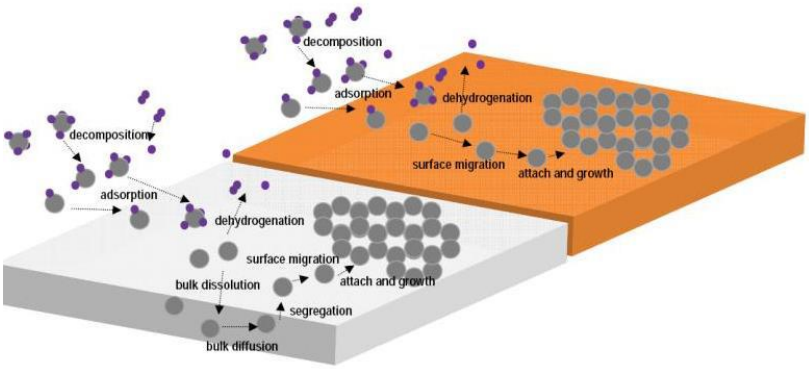

Figure:-8 Growth kinetics in CVD graphene on different catalyst: Case of CH4 on Ni and Cu.

As the graphene synthesis process is a heterogeneous catalytical chemical reaction, the metal performs the two different roles of substrate and catalyst. Therefore, in a typical thermal catalytic CVD, the film grown over metal substrate reduces the catalytic activity due to the catalyst poisoning. This should announce the end of the reaction and the graphene film formation. If the overall process is performed on the surface (adsorption, decomposition and diffusion of molecules), monolayer graphene is preferentially grown. This is known as "self-limiting" effect and was only observed in Cu to date (and also depending on the process conditions). On Ni and other common transition metals (Co, Ru, Ir, etc.,) it was demonstrated that CVD growth of graphene occurs by carbon bulk diffusion due to the high solubility of carbon and segregation (figure 8) during cooling step. In this latter case, solid solution of a mixture of elements is formed near surface and the resulting graphene depends on the kinetic parameters selected for the synthesis. Among all the thermodynamic parameters, a fast cooling rate seems to be a critical factor to suppress the formation of multiple graphene layers [105, 106]. More complex deposition process results when an extra gas phase activation (decomposition by plasma or very high, >1200ºC, temperature) is performed. In this case the chemical reaction evolves to a mixture of heterogeneous catalysis and decomposition in vapour phase. Then the reaction cannot be considered as totally controlled by the catalyst.

The use of carbon isotope labeling technique in conjunction with Raman spectroscopic mapping [107,108] demonstrated effectively different kinetic behavior of CVD growth of graphene on Ni and Cu. By this technique was possible to track carbon during the growth process. The two different mechanisms of graphene growth observed on Ni and Cu can be understood from the C-metal binary phase diagram, being the most important difference that solubility of C in Cu is much lower than that in Ni. Only small amount of carbon can be dissolved on Cu. The source of C is mainly CH4 that is catalytically decomposed on the Cu surface. This route facilitates surface migration and monolayer graphene growth. Experiments with high temperature cycles performed on graphene films of approximately 0.5 monolayer coverage on Cu while continuously imaged using LEEM (Low-Energy Electron Microscopy) confirmed this demonstration. No C precipitation or island growth was observed during cooling in agreement with preliminary reports, suggesting that the process is confined to the surface, with negligible dissolution and precipitation of C from the substrate.

REFERENCE

[1] W. Qian, R. Hao, Y.L. Hou, Y. Tian, C.M. Shen, H.J. Gao and X.L. Liang, Nano Res., 2 (2009) 706.
[2] U. Khan, A. O'Neill, M. Lotya, S. De and J.N. Coleman, Small, 6 (2010) 864.
[3] P. R. Wallace, Phys. Rev. 71 (1947) 622-634
[4] J. C. Slonczewski and P. R. Weiss, Phys. Rev. 109 (1958) 272-279
[5] K. S. Novoselov, A. K. Geim, S. V. Morozov, D. Jiang, Y. Zhang, S. V. Dubonos, I. V. Grigorieva, and A. A. Firsov, Science 306 (2004) 666-669
[6] K. S. Novoselov, Z. Jiang, Y. Zhang, S. V. Morozov, H. L. Stormer, U. Zeitler, J. C. Maan, G. S. Boebinger, P. Kim, and A. K. Geim, Science 315 (2007) 1379-1379
[7] A. Bostwick, T. Ohta, T. Seyller, K. Horn, and E. Rotenberg, Nature Phys. 3 (2007) 36-40
[8] A. K. Geim and K. S. Novoselov, Nature Mater. 6 (2007) 183-191
[9] S. V. Morozov, K. S. Novoselov, M. I. Katsnelson, F. Schedin, D. C. Elias, J. A. Jaszczak, and A. K. Geim, Phys. Rev. Lett. 100 (2008) 016602-016605
[10] K. S. Kim, Y. Zhao, H. Jang, S. Y. Lee, J. M. Kim, K. S. Kim, J.-H. Ahn, P. Kim, J.-Y. Choi, and B. H. Hong, Nature 457 (2009) 706-710
[11] C. Berger, Z. Song, T. Li, X. Li, A. Y. Ogbazghi, R. Feng, Z. Dai, A. N. Marchenkov, E. H. Conrad, P. N. First, and W. A. de Heer, J. Phys. Chem. B 108 (2004) 19912-19916
[12] F. Schedin, A. K. Geim, S. V. Morozov, E. W. Hill, P. Blake, M. I. Katsnelson, K. S. Novoselov, Nature Mater. 6 (2007) 652-655
[13] B. Trauzettel, D. V. Bulaev, L. Loss, and G. Burkard, Nature Phys. 3 (2007) 192-196
[14] C. Berger, Z. M. Song, X. B. Li, X. S. Wu, N. Brown, C. Naud, D. Mayo, T. B. Li, J. Hass, A. N. Marchenkov, E. H. Conrad, P.N. First, and W. A. de Heer, Science 312 (2006) 1191-1196
[15] A. J. van Bommel, J. E. Crombeen, A. van Tooren, Surf. Sci. 48 (1975) 463-472
[16] I. Forbeaux, J.-M. Themlin, and J.-M. Debever, Phys. Rev. B, 58 (1998) 16396-16406
[17] A. Charrier, A. Coati, and T. Argunova, J. Appl. Phys., 92 (2002) 2479-2484

[18] E. Rollings, G.-H.Gweon, S. Y. Zhou, B. S .Mun, J. L. McChesney, B. S. Hussain, A. V. Fedorov, P. N. First, W. A. de Heer, and A. Lanzara, Journal of Physics and Chemistry of Solids 67 (2006)

[19] T. Ohta, A. Bostwick, T. Seyller, K. Horn, and E. Rotenberg, Science 313 (2006) 951-954
[20] J. Hass, W. A.de Heer, and E. H. Conrad, Journal of Physics: Condensed Matter, 20 (2008) 323202(1-27)
[21] W. A. de Heer, C. Berger, X. S. Wu, P. N. First, E. H. Conrad, X. B. Li, T. B. Li, M. Sprinkle, J. Hass, M. L. Sadowski, M. Potemski, and G. Martinez, Solid State Commun., 143 (2007) 92-100
[22] J. Hass, R. Feng, T. Li, X. Li, Z. Zong, W.A. de Heer, P. N. First, E. H. Conrad, C. A. Jeffrey, and C. Berger, Appl. Phys. Lett., 89 (2006) 143106-143108
[23] J. Haas, J. E. Millan-Otoya, M. Sprinkel, W. A. de Heer, C. Berger, P. N. First, L. Magaud, and E. H. Conrad. arXiv:0706.2134
[24] J. Haas, R. Feng, J. E. Millan-Otoya, X. Li, M. Sprinkel, P. N. First, W. A. de Heer, E. H. Conrad, and C. Berger. Phys. Rev. B, 75 (2007) 214109-214116
[25] A. Charrier, A. Coati, T. Argunova, F. Thibaudau, Y. Garreau, R. Pinchaux, I. Forbeaux, J.-M. Debever, M. Sauvage-Simkin, and J.-M. Themlin , J. Appl. Phys. 92 (2002) 2479-2484
[26] T. Ohta, N. C. Bartelt, S. Nie, K. Thürmer, and G. L. Kellogg, Phys. Rev. B 81 (2010) 121411(R) (1-4)
[27] K. V. Emtsev, A. Bostwick, K. Horn, J. Jobst, G. L. Kellogg, L. Ley, J. L McChesney, T. Ohta, S. A. Reshanov, J. Röhrl. E. Rotenberg, A. K. Schmid, D. Waldmann, H. B. Weber and T. Seyller, Nature Mater. 8 (2009) 203-207
[28] R. M. Tromp and J. B. Hannon, Phys. Rev. Lett. 102 (2009) 106104(1-4)
[29] I. Forbeaux, J.-M. Themlin, A. Charrier, F. Thibaudau and J.-M. Debever, Appl. Surf. Sci. 162 (2000) 406-412
[30] J. Hass, F. Varchon, J. E. Millán_otoya, M. Sprinkle, N. Sharma, W. A. de Heer, C. Berger, P. N. First, L. Magaud and E. H. Conrad, Phys. Rev. Lett. 100 (2008) 125504 (1-4)
[31] M. Sprinkle, D. Siegel, Y. Hu, J. Hicks, A. Tejeda, A. Taleb-Ibrahimi, P. Le Fèvre, F. Bertran, S. Vizzini, H. Enriquez, S. Chiang, P. Soukiassian, C. Berger, W. A. de Heer, A. Lanzara, and E. H. Conrad, Phys. Rev. Lett. 103 (2009) 226803 (1-4).

[32] N. Carmara, G. Rius, F. Pérez-Murano, P. Godignon, J-R. Huntzinger, A. Tiberj and J. Camassel, arXiv: 0812.4351v2.
[33] S. Stankovich, D. A. Dikin, G. H. B. Dommett, K. M. Kohlhaas, E. J. Zimney, E. A. Stach, R. D. Piner, S. T. Nguyen, R. S. Ruoff, Nature
2006, 442, 282.
[34] B. C. Brodie, Philos. Trans. R. Soc. London 1959, 149, 249.
[35] L. Staudenmaier, Ber. Deut. Chem. Ges. 1898, 31, 1481.
[36] H. Hamdi, Fortschrittsberichte u¨ber Kolloide und Polymere 1943, 54, 554.
[37] J. William, S. Hummers, R. E. Offeman, J. Am. Chem. Soc. 1958, 80, 1339.
[38] S. Niyogi, E. Bekyarova, M. E. Itkis, J. L. McWilliams, M. A. Hamon,
R. C. Haddon, J. Am. Chem. Soc. 2006, 128, 7720.
[39] M. Hirata, T. Gotou, S. Horiuchi, M. Fujiwara, M. Ohba, Carbon 2004, 42,
2929.
[40] N. I. Kovtyukhova, P. J. Ollivier, B. R. Martin, T. E. Mallouk, S. A. Chizhik,
E. V. Buzaneva, A. D. Gorchinskiy, Chem. Mater. 1999, 11, 771.
[41] T. Nakajima, A. Mabuchi, R. Hagiwara, Carbon 1988, 26, 357.
[42] J. Lu, J.-x. Yang, J. Wang, A. Lim, S. Wang, K. P. Loh, ACS Nano 2009, 3,2367.
[43] H. P. Boehm, A. Clauss, G. O. Fischer, U. Hofmann, Z. Naturforschung1962, 17b, 150.
[44] S. Stankovich, D. A. Dikin, R. D. Piner, K. A. Kohlhaas, A. Kleinhammes,
Y. Jia, Y. Wu, S. T. Nguyen, R. S. Ruoff, Carbon 2007, 45, 1558.
[45] S. Stankovich, R. Piner, S. T. Nguyen, R. S. Ruoff, Carbon 2006, 44, 3342.
[46] A. Lerf, H. He, M. Forster, J. Klinowski, J. Phys. Chem. B 1998, 102, 4477.
[47] H. He, J. Klinowski, M. Forster, A. Lerf, Chem. Phys. Lett. 1998, 287, 53.
[48] L. J. Cote, F. Kim, J. Huang, J. Am. Chem. Soc. 2008, 131, 1043.
[49] D. Cai, M. Song, J. Mater. Chem. 2007, 17, 3678.
[50] J. I. Paredes, S. Villar-Rodil, A. Martı´nez-Alonso, J. M. D. Tasco´n, Langmuir2008, 24, 10560.
[51] H. C. Schniepp, J. L. Li, M. J. McAllister, H. Sai, M. Herrera-Alonso, D. H. Adamson, R. K. Prud'homme, R. Car, D. A. Saville, I. A. Aksay, J. Phys. Chem. B 2006, 110, 8535.
[52] S. Stankovich, R. D. Piner, X. Q. Chen, N. Q. Wu, S. T. Nguyen, R. S. Ruoff,J. Mater. Chem. 2006, 16, 155.
[53] M. J. McAllister, J. L. Li, D. H. Adamson, H. C. Schniepp, A. A. Abdala, J. Liu, M. Herrera-Alonso, D. L. Milius,
[54] G. Eda, M. Chhowalla, Nano Lett. 2009, 9, 814.
[55] X. Sun, Z. Liu, K. Welsher, J. T. Robinson, A. Goodwin, S. Zaric, H. Dai, Nano Res. 2008, 1, 203.
[56] G. Eda, G. Fanchini, M. Chhowalla, Nat. Nanotechnol. 2008, 3, 270.
[57] M. Hirata, T. Gotou, S. Horiuchi, M. Fujiwara, M. Ohba, Carbon 2004, 42,2929.
[58] L. J. Cote, F. Kim, J. Huang, J. Am. Chem. Soc. 2008, 131, 1043.[59] D. Li, M. B. Mu¨ller, S. Gilje, R. B. Kaner, G. G. Wallace, Nat. Nanotechnol. 2008, 3, 101.
[60] I. Jung, M. Vaupel, M. Pelton, R. Piner, D. A. Dikin, S. Stankovich, J. An, R. S. Ruoff, J. Phys. Chem. C 2008, 112, 8499.
[61] A. Buchsteiner, A. Lerf, J. Pieper, J. Phys. Chem. B 2006, 110, 22328.
[62] H.-K. Jeong, Y. P. Lee, M. H. Jin, E. S. Kim, J. J. Bae, Y. H. Lee, Chem. Phys.Lett. 2009, 470, 255.
[63] P. Blake, E. W. Hill, A. H. C. Neto, K. S. Novoselov, D. Jiang, R. Yang, T. J. Booth, A. K. Geim, Appl. Phys. Lett. 2007, 91, 063124.
[64] D. S. L. Abergel, A. Russell, V. I. Fal'ko, Appl. Phys. Lett. 2007, 91, 063125.
[65] I. Jung, M. Pelton, R. Piner, D. A. Dikin, S. Stankovich, S. Watcharotone, M. Hausner, R. S. Ruoff, Nano Lett. 2007, 7, 3569.

[66] E. Treossi, M. Melucci, A. Liscio, M. Gazzano, P. Samorı `, V. Palermo, J. Am. Chem. Soc. 2009, 131, 15576.
[67] J. Kim, L. J. Cote, F. Kim, J. Huang, J. Am. Chem. Soc. 2009, 132, 260.
[68] L. Zhang, J. Liang, Y. Huang, Y. Ma, Y. Wang, Y. Chen, Carbon 2009, 47,3365.

[69] C.-Y. Su, Y. Xu, W. Zhang, J. Zhao, X. Tang, C.-H. Tsai, L.-J. Li, Chem. Mater. 2009, 21, 5674.

[70] C. Go´mez-Navarro, T. R. Weitz, A. M. Bittner, M. Scolari, A. Mews, M. Burghard, K. Kern, Nano Lett. 2007, 7, 3499.

[71] S. Gilje, S. Han, M. Wang, K. L. Wang, R. B. Kaner, Nano Lett. 2007, 7,3394.
[72] S. Park, R. S. Ruoff, Nat. Nanotechnol. 2009, 4, 217.
[73] K. P. Loh, Q. Bao, P. K. Ang, J. Yang, J. Mater. Chem. 2010, DOI: 10.1039/ b920539.
[74] V. C. Tung, M. J. Allen, Y. Yang, R. B. Kaner, Nat. Nanotechnol. 2009, 4, 25.
[75] A. B. Bourlinos, D. Gournis, D. Petridis, T. Szabo, A. Szeri, I. Dekany, Langmuir 2003, 19, 6050.
[76] Y. Si, E. T. Samulski, Nano Lett. 2008, 8, 1679.
[77] H.-J. Shin, K. K. Kim, A. Benayad, S.-M. Yoon, H. K. Park, I.-S. Jung, M. H. Jin, H.-K. Jeong, J. M. Kim, J.-Y. Choi, Y. H. Lee, Adv. Funct. Mater 2009, 19, 1987.
[78] J. Shen, Y. Hu, M. Shi, X. Lu, C. Qin, C. Li, M. Ye, Chem. Mater. 2009, 21,3514.
[79] N. Mohanty, A. Nagaraja, J. Armesto, V. Berry, Small 2009, 6, 226.
[80] G. X. Wang, J. Yang, J. Park, X. L. Gou, B. Wang, H. Liu, J. Yao, J. Phys.Chem. C 2008, 112, 8192.
[81] Y. Chen, X. Zhang, P. Yu, Y. Ma, Chem. Commun. 2009, 4527.
[82] X. Fan, W. Peng, Y. Li, X. Li, S. Wang, G. Zhang, F. Zhang, Adv. Mater.2008, 20, 4490.
[83] Y. Zhou, Q. Bao, L. A. L. Tang, Y. Zhong, K. P. Loh, Chem.Mater. 2009, 21, 2950.
[84] E. Matuyama, J. Phys. Chem. 2002, 58, 215.
[85] X. Li, H. Wang, J. T. Robinson, H. Sanchez, G. Diankov, H. Dai, J. Am.Chem. Soc., 2009, 131, 15939.
[86] V. Lee, L. Whittaker, C. Jaye, K. M. Baroudi, D. A. Fischer, S. Banerjee,Chem. Mater. 2009, 21, 3905.
[87] W. Gao, L. B. Alemany, L. Ci, P. M. Ajayan, Nat. Chem. 2009, 1, 403.
[88] Z. Ming,W. Yuling, Z. Yueming, Z. Junfeng, R. Wen, W. Fuan, D. Shaojun,Chem. Eur. J. 2009, 15, 6116.
[89] G. K. Ramesha, S. Sampath, J. Phys. Chem. C 2009, 113, 7985.
[90] Z. Wang, X. Zhou, J. Zhang, F. Boey, H. Zhang, J. Phys. Chem. C 2009, 113,14071.
[91] G. Williams, B. Seger, P. V. Kamat, ACS Nano 2008, 2, 1487.
[92] X. Wang, L. Zhi, K. Mu¨llen, Nano Lett. 2008, 8, 323.
[93] H. A. Becerill, J. Mao, Z. Liu, R. M. Stoltenberg, Z. Bao, Y. Chen, ACS Nano2008, 2, 463.
[94] L. J. Cote, R. Cruz-Silva, J. Huang, J. Am. Chem. Soc. 2009, 131, 11027.
[95] K. S. Novoselov, D. Jiang, F. Schedin, T. J. Booth, V. V. Khotkevich,S. V. Morozov, and A. K. Geim, Two-dimensional atomic crystals, PNAS, 102, 10451 (2005).
[96] A.K. Geim., Graphene: Status & Prospects. Sci.324: 1530-34 (2009).
[97] P.R. Somani, S.P. Somani, and M. Umeno., Planer nanographenes from camphor by CVD, Chemical Physics Letters, 430, 56 (2006).
[98] Li, X et al. Large-area synthesis of high-quality and uniform graphene films on copper foils. Science 324, 1312-1314 (2009).
[99] Bae, S. et al. Roll-to-roll production of 30-inch graphene films for transparent electrodes. Nat Nanotech. 5, 574 (2010).
[100]MOROSANU, C. E.: "Thin Films by Chemical Vapour Deposition", Elsevier
[101]SHERMAN, A.: "Chemical Vapor Deposition for Microelectronics". Noyes Publications
[102]PIERSON, H. O.: "Handbook Of Chemical Vapour Deposition". Noyes Publications.
[103]HUIMIN, L.: "Diamond Chemical Vapour Deposition". Noyes Publications.
[104]RICKERBY, D. S: "Advanced Surface Coatings". Blackie.
[105]SCHUEGRAF, K. K.: "Handbook Of Thin-film Deposition Processes and Techniques", Noyes Publications.
[106] Albella J.M, "Láminas Delgadas y Recubrimientos. Preparación, propiedades y aplicaciones. CSIC, 2003.
[107] Lenzsolomun P, Wu MC, Goodman W. Methane coupling at low-temperatures on Ru(0 0 0 1) and Ru-11(2) bar-0 catalysts. Catal Lett 1994; 25: 75–86.
[108] Alfonso Reina, Xiaoting Jia, John Ho, Daniel Nezich, Hyungbin Son, Vladimir Bulovic, Mildred S. Dresselhaus and Jing Kong. Large Area, Few-Layer Graphene Films on Arbitrary Substrates by Chemical Vapor Deposition. Nanoletters 2009, 9, 30-35
[109] Keun Soo Kim, Yue Zhao, Houk Jang, Sang Yoon Lee, Jong Min Kim, Kwang S. Kim, Jong Hyun Ahn, Philip Kim, Jae-Young Choi & Byung Hee Hong. Large-scale pattern growth of graphene films for stretchable transparent electrodes. Nat. letters. 457, 706 (2009)
[110] Xuesong Li, Weiwei Cai, Luigi Colombo and Rodney S. Ruoff. Evolution of Graphene Growth on Ni and Cu by Carbon Isotope Labeling. NANOLETTERS 2009 Vol. 9, No. 12, 4268-4272
[111] Martin Kalbac, Otakar Frank, Ladislav Kavan. The control of graphene double-layer formation in copper catalyzed chemical vapor deposition. CARBON 50(2012) 3682-3687
[112] Joseph M. Wofford, Shu Nie, Kevin F. McCarty, Norman C. Bartelt and Oscar D. Dubon Graphene Islands on Cu Foils: The Interplay between Shape, Orientation, and Defects. Nano Lett. 2010, 10, 4890-4896